

An upper limit on electron antineutrino mass from Troitsk experiment

V.N. Aseev, A.I. Belesev, A.I. Berlev, E.V. Geraskin, A.A. Golubev, N.A. Likhovid, V.M. Lobashev, A.A. Nozik, V.S. Pantuev, V.I. Parfenov, A.K. Skasyrskaya, F.V. Tkachov, S.V. Zadorozhny
Institute for Nuclear Research of Russian Academy of Sciences, Moscow, Russia

(Dated: May 22, 2018)

An electron antineutrino mass has been measured in tritium β -decay in the Troitsk ν -mass experiment. The setup consists of a windowless gaseous tritium source and an electrostatic electron spectrometer. The whole data set acquired from 1994 to 2004 was reanalyzed. A thorough selection of data with the reliable experimental conditions has been performed. We checked every known systematic effect and obtained the following experimental estimate for neutrino mass squared $m_\nu^2 = -0.67 \pm 2.53 \text{ eV}^2$. This gives an experimental upper sensitivity limit of $m_\nu < 2.2 \text{ eV}$, 95% *C.L.* and upper limit estimates $m_\nu < 2.12 \text{ eV}$, 95% *C.L.* for Bayesian statistics and $m_\nu < 2.05 \text{ eV}$, 95% *C.L.* for the Feldman and Cousins approach.

PACS numbers: 14.60.Lm, 14.60.Pq, 23.40.-s

I. INTRODUCTION

The standard model of particle physics assumes zero mass for all neutrino flavors. However, the discovery of neutrino oscillations in experiments with solar, atmospheric and reactor neutrinos gives a strong evidence of a nonzero neutrino mass [1]. Oscillation parameters allow one to estimate the difference of mass squared values which give only the lower limit on neutrino eigenstate masses. The question of absolute values is still open. The most attractive methods to obtain an absolute mass value are neutrinoless double betadecay ($2\beta0\nu$) in even - even parity transitions in some nuclei (the probability of such a process depends on neutrino mass) and the method which measures the highest edge of electron energy spectrum in β decay. In the former case, the decay is possible only if neutrinos are of the Majorana type, while in the latter case the experiment gives a model independent estimation of electron antineutrino mass irrespective of its type, Majorana or Dirac.

The measurement of the electron spectrum in tritium β decay is one of the most precise direct measurements of neutrino mass. This type of measurements was utilized in the Troitsk and Mainz experiments. In 2003 the Troitsk group, having analyzed about half of the accumulated statistics, presented the upper limit for the neutrino mass at 95% $m(\nu_e) < 2.05 \text{ eV}$ [2]. This result was obtained by excluding some additional small structure with unclear origin close to the spectrum end point. The Mainz group in 2005 published the final result of their search for neutrino mass [3]. They measured an upper limit of $m(\nu_e) \leq 2.3 \text{ eV}$.

In the paper we present a complete result of the Troitsk ν -mass experiment. We reexamined the whole set of measurements reassessing the data quality and our knowledge of all the experimental conditions. Measurements with unstable or unclear conditions were removed. Some of the experimental corrections were reexamined. For each run of measurements we evaluated with the best known precision different experimental parameters, in particular, column density in a gaseous tritium source. In the

current analysis we used a new method of quasioptimal weights [4] to fit the measured electron spectrum. The obtained results were also compared with the standard fitting procedure based on the MINUIT package [5]. The two methods agree within statistical errors.

The paper is organized as follows: in Sec. II we briefly describe the experimental setup and measurement procedure. Analysis details are presented in Sec. III. In Sec. IV we describe systematic uncertainty. The final results are presented in Sec. V, and in Sec. VI we conclude.

II. EXPERIMENTAL SETUP AND PROCEDURE OF MEASUREMENTS

A. Experimental Setup

The choice of tritium as a β decay source is guided by its long half-life time (about 12.3 years), which guarantees a long stability during the measurement time. Relatively low energy (the maximum electron energy is about 18.6 keV) makes it possible to use an electrostatic spectrometer. The simplicity of electron shells in molecular tritium allows one to calculate corrections on excited states in the molecules T^3He or H^3He , which are produced as final states after the decay. The Troitsk experiment has two major features: the β spectrum was measured by an integrating electrostatic spectrometer with adiabatic magnetic collimation, and a windowless gaseous tritium source (WGTS) [6] was used as a volume for β decays. The spectrometer allows one to get resolution of 3-4 eV, while the WGTS minimizes distortions of the electron spectrum. The setup is shown in Fig. 1, and details can be found in [2].

Tritium gas is injected into a long pipe of WGTS in the axial magnetic field of about 0.8 T, where tritium partially decays. At both ends of the pipe there are superconducting coils which form magnetic plugs with a field up to 5 T. The reason for this magnetic field configuration was to avoid electron acceptance from tritium decays from the pipe wall. Electrons are transported

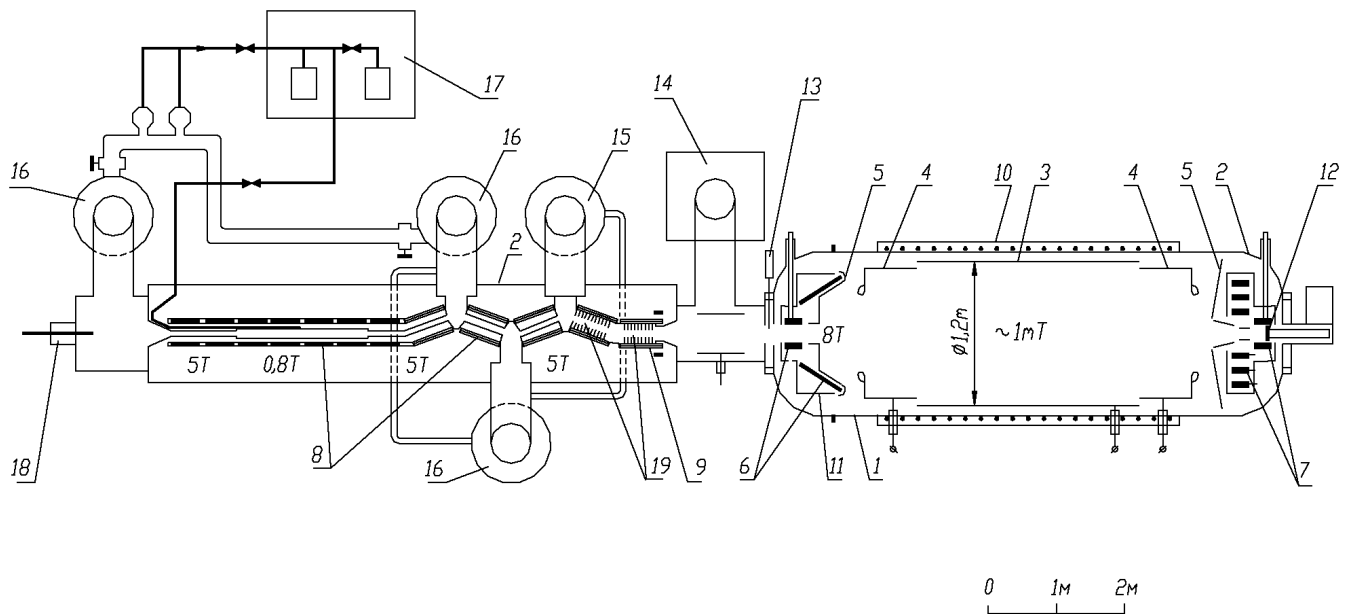


FIG. 1: Diagram of the installation: 1,2 – vacuum volume; 3,4 – electrostatic system; 5 – ground electrode; 6-9 – superconducting coils; 10 – warm solenoid; 11 – Nitrogen shield; 12 – Si(Li) detector; 13 – emergency valve; 14 – magneto-discharge pump; 15,16 – mercury diffusion pumps; 17 – tritium purification system; 18 – electron gun; 19 – argon trap.

via a zigzag-type transport system to the spectrometer, while residual gas and ions are pumped by a differential pumping system. After some purification the gas returns again to the pipe.

At the entrance of the spectrometer the magnetic field is formed by superconducting coils of $B_{max} = 8\text{ T}$; in the middle of the spectrometer the magnetic field drops to about $B_{min} \approx 1\text{ mT}$. Magnetic field lines are collected again by a 3 T magnet with a Si(Li) counter inside. This configuration of the magnetic field collimates electrons in such a way that a transverse component of the electron momentum becomes small near the middle of the spectrometer (analyzing plane) and the electron angular distribution along the spectrometer axis is limited by a small value of $\delta = B_{min}/B_{max}$. In the analyzing plane there is also a strong electrostatic retarding field oriented against the electron direction. Only the electrons with energy above the retarding field will pass the barrier, while all the other electrons with smaller energy will be reflected. By changing the electrostatic potential we can scan and get an integrated electron spectrum.

Electrons at the far end of the spectrometer are counted by an Si(Li) detector with a sensitive area of about 17 mm in diameter. The signal amplitude and its arrival time are digitized and readout by a computer and online KAMAK electronics with a fixed dead time of 7.2 μsec .

B. Procedure

The measurement procedure was as follows: the integrated yield of β -electrons near the end point of the spectrum was scanned by changing the electrostatic potential in the spectrometer to a range between 18000 and 18900 volts. There were 60-80 set points with a measurement time of 10 to 200s depending on the count rate at the set point. The sequence of points in potential values was forward and reverse and random as well. To control the intensity in the WGTS, every 15min there was a monitor point measurement at 18000 V, where the counting rate is large.

The data format was as follows: at the beginning of each scan we checked the readiness of the electronics and the high voltage system. Then we started the scan by varying the electrostatic potential. For each set point high voltage was checked to be within 0.2V of the required value. The value of this deviation was checked every second and recorded in the file for further offline corrections. At the end of each scan we wrote the pressure in the WGTS and started the next set in the opposite direction.

During the measurements we controlled and recorded the temperatures of cooling helium and superconducting magnets. About every 2h we measured hydrogen isotope concentrations in the WGTS.

III. DATA ANALYSIS

A. Data selection and experimental corrections

During the preliminary data selection and analysis we checked the consistency of the mean count rate at each set point. Analysis shows that there are increases of the counting rate. This effect is induced by a local discharge from tritium decays inside the spectrometer (there is a small but finite probability for molecules from the WGTS to penetrate to the spectrometer) or from electrons which escape from magnetic “traps” inside the spectrometer. A special algorithm was developed to find these bunches and exclude that time interval from the analysis. After that, we checked the distribution of time intervals between events, which followed the Poisson distribution and looked like a pure exponentially falling distribution. At set points where the intensity was large and it was hard to distinguish such bunches, we extrapolated from points with a low counting rate.

Data were corrected for signal pileup and for electronics dead time. In the final analysis we used points only above 18400 V, where these corrections are small, except for the monitor points at 18000 V.

Files with a full set of measurements were then checked for stability of the counting rate at the monitor point within 10% from the average value. This allows one to control the stability of isotope contents in the WGTS, avoiding a sudden change caused by the purification system. Points with large high voltage offsets were also removed. Special care was taken to keep only the runs where precise measurements of the column density in the WGTS were performed (see below).

B. Method of quasioptimal weights

The fit of parameters in the previous analysis [2] was done by means of the standard MINUIT package which uses the method of least squares. Yet the effectiveness of such a method of parameter estimation is not guaranteed at a low number of counts where the distribution is Poissonic rather than Gaussian. To account for that problem a method of quasioptimal weights in Ref. [4] was implemented. This quite general procedure uses a well-known method of moments as a basis. The method of moments is simple, reliable, and analytically transparent, but its effectiveness can be low. A way to eliminate the latter drawback was described in the same article [4]. The general scheme of the method is as follows.

First one has to choose weight functions $\phi_i(X_i)$ of measured values X_i (in our case X_i are count numbers for different retarding potentials on the electrode). Then one should calculate the weighted average for the data set and the corresponding average over the fitting curve, which depends on the parameters θ being estimated:

$$\begin{aligned}\langle\phi\rangle_{\text{exp}} &= \frac{1}{N} \sum_{i=1}^N \phi_i(X_i), \\ \langle\phi\rangle_{\text{th}} &= \frac{1}{N} \sum_{i=1}^N \langle\phi_i(\theta)\rangle_{\text{th}},\end{aligned}\quad (1)$$

where N is the number of points in the file.

Requiring $\langle\phi\rangle_{\text{exp}} = \langle\phi\rangle_{\text{th}}$, we get equations on θ . If one gets a number of different weights ϕ (equal to the number of parameters θ), it is possible to get the system of equations, whose solution is the estimate of θ . Variation of $\langle\phi\rangle_{\text{th}}$ gives error estimation for parameters. As for the choice of weights, there is a simple explicit formula for optimal weight, which gives minimal variation of estimation of parameters (Rao-Cramer bound). This formula involves the unknown values of θ , but deviation of variance from the Rao-Cramer minimum is quadratic with respect to the deviation of weights from the optimal expression; thus it makes practical sense to use not the exact optimal weights based on unknown “real” values of parameters, but quasioptimal ones based on parameter values that are close to the “real” ones. A poor choice of the weight would not affect the consistency of the method, but the variance would be larger than for the optimal weight; in other words, the resulting estimate would be suboptimal but still correct.

Efficiency of the method and stability of its program implementation (a robust code written in statically type-safe component pascal) were tested by comparison with the most commonly used methods. Statistical tests showed that the efficiency of the method of quasioptimal weights is equal to that of the method of maximum likelihood (which is known to give the best effectiveness in such cases). Direct comparison of the parameter obtained using MINUIT (the JMINUIT package was used [7]) to the quasioptimal weights method showed no discrepancies, within the calculation uncertainties.

C. Spectrum and corrections

In our experiment we measured an integrated electron spectrum. Thus, we have to start with an unmodified theoretical β spectrum of tritium decay and integrate it with experimental resolution. The spectrum is also distorted by electron interactions in the WGTS. There is also another set of corrections, and as a result, the analysis has several steps.

The electron energy spectrum in β decay is described by the following wellknown expression:

$$\begin{aligned}S(E, E_0, m_\nu) &= N \cdot F(Z, E) \cdot (E + m_e) \cdot p \cdot (E_0 - E)^2 \\ &\times \sqrt{1 - \frac{m_\nu^2}{(E_0 - E)^2}}\end{aligned}\quad (2)$$

where E , p , and m_e are the electron kinetic energy, momentum, and mass; m_ν is the neutrino mass; E_0 is the spectrum energy edge in the case $m_\nu = 0$; N is the normalization constant and $F(Z, E)$ is the so-called Fermi function, which induces an electrostatic correction to the charge Z of the residual nucleus [8].

Equation 2 depends on m_ν^2 , and the preliminary analysis of both experiments, Troitsk and Mainz, has shown that experimental estimations on m_ν^2 may get negative values. Besides statistical fluctuations, such behavior could be attributed to some experimental systematics with unknown origin which moves the spectrum end point beyond its maximum value E_0 . To account for this effect, Eq. 2 should be extended to negative ranges of m_ν^2 . We also checked different methods of such an extension and found a weak dependence of the result on the actual choice. Finally, we chose the method used in the Mainz experiment [3].

Often after the decay of a tritium nucleus, the final molecule T^3He will not go to its ground state; thus, we have to sum over all final states i , and Eq. 2 should be replaced by the sum

$$S(E) = \sum_i N(E, E_0 - E_i) \cdot P_i, \quad (3)$$

where E_i is energy of the excited state and P_i is its probability. The summation is done over the excited spectrum divided into a set of narrow bins, as shown in Fig. 2, keeping the sum of P_i equal to 1. Unfortunately, this

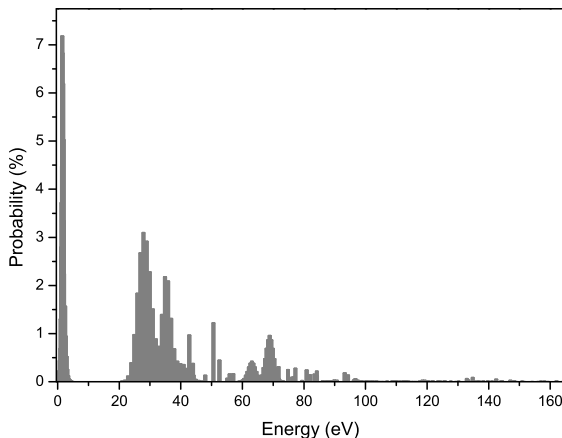


FIG. 2: Final states spectrum in molecule T^3He [9]. Every bin is a summand in eq. 3.

spectrum was not measured experimentally with good accuracy; thus, we have to use theoretical model calculations. We use a generated spectrum from Ref. [9]. For comparison, we also checked a few other models and found that a final result on the square value of the neutrino mass does not change much and stays within our estimation of the total systematic uncertainty.

Electrons in the WGTS suffer from scattering on tritium molecules. To account for such an effect, we have to convolute Eq. 3 with the energy loss function. We use a detailed analysis of this function, which was performed in [10]. In Fig. 3 we show the electron energy loss spectrum in tritium for single, double, and triple scattering. The results for double and triple scattering were calculated as a convolution of a single loss spectrum with itself.

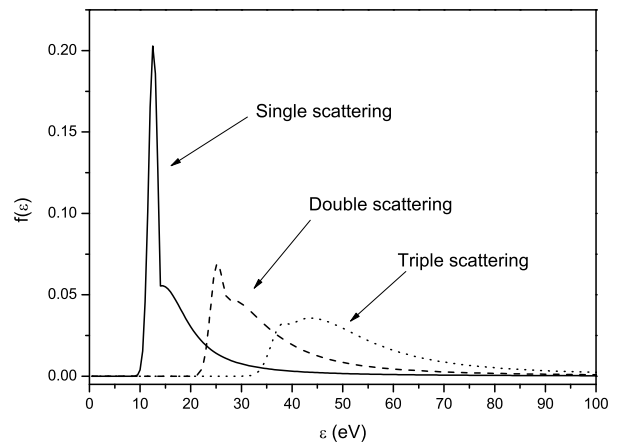


FIG. 3: The shape of the electron energy loss spectrum in tritium [10]. Different curves correspond to electron single, double, and triple scattering.

Multiple scattering should follow the Poisson distribution; thus, we can write the probability for scattering of the order of k as

$$P_k = \frac{X^k e^{-X}}{k!}. \quad (4)$$

Here $X = \int_0^L \frac{dl}{\lambda(l)} = \int_0^L \sigma_{tot} n(l) dl$ is the ratio of the electron path length in the gas to a mean free path, where L is the pass length, $n(l)$ is the gas density at point l , and σ_{tot} is the total inelastic cross section. In practice, in our calculations we considered up to the triple scattering processes only: at a typical value of $X = 0.35$, $P_4 = 0.00044$.

Electrons produced in different parts of the WGTS have different X , and so we average each value of P_k over the path length. This averaging may be performed analytically. Suppose all electrons move exactly along the magnetic field lines which in the WGTS are directed along its length. In a volume element of the pipe, Sdl , the number of molecules is $dN = Sn(l)dl$, where S is the pipe cross section, n —the gas density, and l —the coordinate along the pipe. If $dX = \sigma_{tot} n(l) dl$, then $dN = S/\sigma_{tot} n(l) dX = C \cdot dX$, where C is a constant. The average probability for a path with no scattering will

be

$$\langle P_0 \rangle = \frac{C \int_0^{N_{tot}} e^{-X} dN}{C \int_0^{N_{tot}} dN} = \frac{\int_0^{X_0} e^{-X} dX}{\int_0^{X_0} dX} = \frac{1}{X_0} (1 - e^{-X_0}). \quad (5)$$

Here X_0 is the total length expressed in units of the mean free path. In a similar way we get

$$\begin{aligned} \langle P_1 \rangle &= \frac{1}{X_0} (1 - e^{-X_0}) - e^{-X_0}, \\ \langle P_2 \rangle &= \frac{1}{2X_0} (2 - e^{-X_0} (X_0^2 + 2X_0 + 2)), \\ \langle P_3 \rangle &= \frac{1}{6X_0} (6 - e^{-X_0} (X_0^3 + 3X_0^2 + 6X_0 + 6)). \end{aligned} \quad (6)$$

In addition, we have to take into account electron circular motion which increases electron path length while they are moving in the magnetic field. This increase depends on the orientation of the electron momentum vector relative to the magnetic field direction. The magnetic field does not change the absolute value of the electron velocity V , but changes its direction, keeping the velocity longitudinal component V_z constant. Thus, we can write the expression for time which is needed for the electron to cover a distance z along the pipe as $t = z/V_z$. The total electron path is $D = V \cdot t$, and we can write

$$\frac{X}{X_0} = \frac{D}{z} = \frac{V}{V_z} = \frac{1}{\cos \theta}, \quad (7)$$

where $\cos \theta$ is the angle between the electron velocity and the magnetic field direction.

We calculated P_i taking into account the fact that only a fraction of electrons will pass to the spectrometer. The results for corrections on electron magnetic winding were approximated by linear functions:

$$\begin{aligned} P_0 &= \langle P_0 \rangle \cdot (0.9996 - 0.0398 \cdot X_0), \\ P_1 &= \langle P_1 \rangle \cdot (1.0854 - 0.0460 \cdot X_0), \\ P_2 &= \langle P_2 \rangle \cdot (1.1595 - 0.0567 \cdot X_0), \\ P_3 &= \langle P_3 \rangle \cdot (1.2398 - 0.0682 \cdot X_0). \end{aligned} \quad (8)$$

Strictly speaking, the linear approximation is our arbitrary choice, but as we have found, the contribution of higher orders is less than 0.05% for our range of the parameter X_0 .

Direct measurement of gas density in the WGTS pipe with the required precision is impossible. During data taking, for each file we measure the intensity in the monitoring point at the spectrometer potential $U = 18000$ V. At such a voltage, a significant portion of the electron spectrum will pass the spectrometer with a relatively large counting rate N_{mon} . This rate is proportional to the total amount of tritium in the source pipe. An additional mass analyzer directly connected to the WGTS, at the same time measures partial concentrations of T_2 , TH, and H_2 molecules. From this measurement we calculate the ratio P_T of tritium atoms to the total number

of hydrogen isotope atoms. Introducing an additional calibration constant A , we can write the relation

$$X_0 = A \cdot \frac{N_{mon}}{P_T}. \quad (9)$$

The calibration constant A depends on many experimental conditions, such as magnetic field configuration or temperature in the pipe, but during a particular run, it remains constant within the systematic uncertainties. We find the value of A experimentally using an electron gun mounted at the rear end of the WGTS. The gun produces a monochromatic beam of electrons in the energy range of up to 20 keV which pass through the whole WGTS pipe. With no gas in the pipe the gun allows us to measure the transition function or resolution of the spectrometer. When the pipe is filled with gas the integrated spectrum from the gun in the spectrometer changes, Fig. 4. There is a sharp edge of the spectrum to

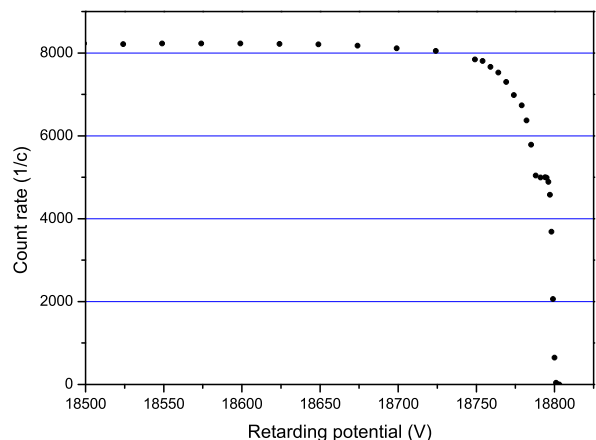


FIG. 4: Integrated spectrum from the electron gun versus the applied potential on the spectrometer electrode. The WGTS pipe is filled with tritium. The voltage on the electron gun cathode is around 18800 V.

the right located at the gun potential. To the left of this edge, first we see a flat step with a width of about 12 V, which corresponds to electrons with no scattering in the pipe. Then, there is another rise from electrons which lost at least 12 eV after a single scattering, compare this behavior with the energy loss spectrum in Fig. 3. The integral of the spectrum at spectrometer potential values below 200 from the right edge corresponds to all electrons with or without scattering. The ratio of the magnitude of the right step to the total number of electrons in the left part of the spectrum is equal to the probability with no scattering, which is related to X_0 . Taking into account the correction for track winding for electrons from the gun we can solve Eq. 9 for parameter A . Such calibration measurements for parameter A were performed for each run. The runs which did not have these calibrations were rejected.

At an early stage of the experiment we found that there is an additional contribution to the spectrum from electrons which are trapped in the WGTS. More than 90% of β electrons which were produced at a large angle relative to the axial magnetic field cannot escape because of strong fields which work as magnetic plugs at both ends of the WGTS. In the adiabatic regime the maximum electron angle relative to the magnetic field for the electrons to escape through the plug can be found from

$$\sin \alpha_{max} = \sqrt{\frac{B_S}{B_T}} = \sqrt{\frac{0.8}{5}} = 0.4, \quad (10)$$

where B_S is the field in the pipe and B_T is the field in the transport system. Thus we get $\alpha_{max} = 23.5^\circ$.

Trapped electrons suffer from multiple reflections from the magnetic plugs. In general, they cannot escape the trap. However, electrons may scatter on molecules in the WGTS, change their angle relative to the magnetic field, and be transported to the spectrometer. Such an effect is electron diffusion in the surrounding gas to the transport system phase space. The portion of these electrons which reaches the spectrometer is only about 10^{-4} from the electrons within the acceptance. Nevertheless, we have to account for this effect because the energy loss spectrum for trapped electrons is very different. We did Monte Carlo simulation for tritium decays in the WGTS. The total number of the generated electrons was 10^7 , the number of electrons which finally got to the spectrometer was 9800. In Fig. 5 we show the energy loss spectrum for these electrons. Simulated results were approximated by

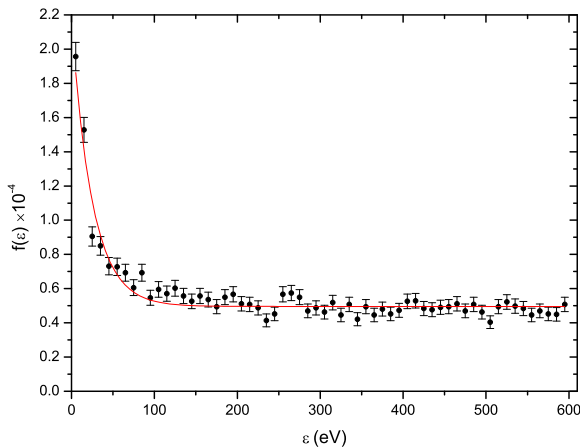


FIG. 5: Energy loss spectrum, $\varepsilon = E_{in} - E_{fin}$, for electrons which were trapped in WGTS but after scattering reached the spectrometer. The bin size is 10 eV. The solid line is the analytic approximation of the losses.

an analytic function

$$trap(\varepsilon) = 1.86 \cdot 10^{-4} \cdot \exp\left(-\frac{\varepsilon}{25}\right) + 5.5 \cdot 10^{-5} \quad (11)$$

shown by a solid line in Fig. 5. The final energy loss function could be written as

$$Tr(\varepsilon) = P_0\delta(\varepsilon) + P_1f_1(\varepsilon) + P_2f_2(\varepsilon) + P_3f_3(\varepsilon) + trap(\varepsilon), \quad (12)$$

where P_i are mean probabilities to scatter i times from Eq. 8 and $f_i(\varepsilon)$ are energy loss distribution functions for i th scattering.

The electron spectrum should be integrated with a resolution function which is defined by the following equation [10]:

$$R(U, E) = \begin{cases} 0 & E - U < 0, \\ \frac{1 - \sqrt{1 - \frac{E-U}{E} \frac{B_S}{B_A}}}{1 - \sqrt{1 - \frac{\Delta E}{E} \frac{B_S}{B_A}}} & 0 \leq E - U \leq \Delta E, \\ 1 & E - U \geq \Delta E, \end{cases} \quad (13)$$

where E is the electron energy, U is the spectrometer electrode potential, $\Delta E = \frac{B_S}{B_0}E$, B_A is the magnetic field in the spectrometer analyzing plane, B_S is the magnetic field in the WGTS pipe, and B_0 is the field in the pinch magnet at the entrance of the spectrometer.

We use this analytic form for the resolution function which depends only on field configurations. To justify the validity of Eq.13, we performed a full simulation with the nominal electrostatic and magnetic fields in the realistic geometry. We found that an analytic representation of the transmission function by Eq.13 describes very well results of the simulation. The experimental resolution, or transmission function, was also measured with the electron gun and the results agree with the theoretical estimate with errors which are determined based on the stability of the high voltage system. These errors are treated as systematic uncertainties. The resolution function is shown in Fig. 6 and looks almost linear.

Finally, we get the following expression for the experimental integrated electron spectrum:

$$Sp(U) = N \cdot \int [S(E, E_0, m_\nu^2) \otimes Tr(E)] \cdot R(U, E) dE + bkgr, \quad (14)$$

where $S(E, E_0, m_\nu^2)$ is the electron spectrum from β decay [Eq. 3], $Tr(E)$ is the energy loss spectrum [Eq. 12], $R(U, E)$ is the resolution function [Eq. 13], and bkgr is experimental background.

In the data analysis we use four free parameters: m_ν^2 , E_0 —the spectrum energy edge for the case $m_\nu = 0$, N —the normalization constant and bkgr.

D. Summing-up files

Each data file was measured within about 2 h. During one run of measurements an effective column density in the WGTS may vary by 10% from file to file. To add files with different density we use the following procedure (for

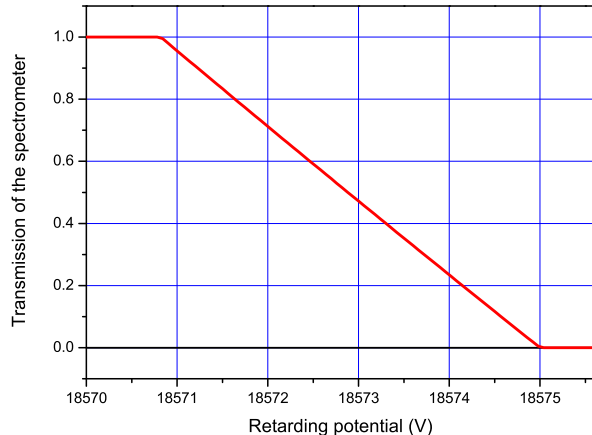


FIG. 6: Resolution function for electrons with energy of 18575 eV. The curve corresponds to the magnetic field ratio $B_A/B_0=2.26 \cdot 10^{-4}$.

simplicity we present an example for two files):

$$\begin{aligned}
 Sp_1(U) + Sp_2(U) &= N_1 \int S(E) \otimes Tr_1 \cdot R(U, E) dE \\
 &\quad + N_2 \int S(E) \otimes Tr_2 \cdot R(U, E) dE \\
 &= \int S(E) \otimes (N_1 Tr_1 + N_2 Tr_2) \cdot R(U, E) dE \\
 &= 2 \int S(E) \otimes \left(\frac{N_1 \cdot P_0^1 + N_2 \cdot P_0^2}{2} \delta(\varepsilon) \right. \\
 &\quad \left. + \frac{N_1 \cdot P_0^2 + N_2 \cdot P_0^1}{2} f(\varepsilon) + \dots \right) \cdot R(U, E) dE, \quad (15)
 \end{aligned}$$

where N_1 and N_2 are normalization constants for each file from a fit by Eq. 14. In this procedure, over many files, we actually average probabilities for multiple scattering:

$$P_i = \frac{\sum_{j=1}^n P_i^j \cdot N^j}{\sum_{j=1}^n N^j} \quad (i = 0 - 3). \quad (16)$$

IV. SYSTEMATIC ERRORS

The main source of systematic uncertainties is the uncertainty in the estimation of the WGTS column thickness X_0 . During one run the value of the source thickness is constantly varying (in the bounds of 5%-10% from the mean value). For each data file with a duration of 2-2.5 h, X_0 was measured using Eq. 9. The error of the count rate in the monitor point is negligibly small (less than 0.1%). The error for the tritium concentration mainly comes from its drift during the file (about 1.5%). The error for coefficient A is calculated from its estimation procedure and is 1.5%. Therefore, we use 3% as a conservative error of X_0 .

The second contribution to the systematic uncertainty comes from the final state spectrum of $T^3\text{He}$, Fig. 2. As mentioned above, there is no direct experimental measurements of this spectrum, and we have to use theoretical estimates. The influence of the uncertainty in the final state spectrum was investigated in [2] and was found to be 0.7 eV^2 in the neutrino mass squared determination.

The error in the trapping-effect estimation arises from the uncertainty in the cross sections of the electron interaction with a tritium molecule. This error was taken as 20% of the full amplitude of the trapping effect. The influence of this error on the neutrino mass squared is calculated individually for each run and varies within $0.3\text{-}0.5 \text{ eV}^2$.

An additional uncertainty comes from the instability of the potential on the main spectrometer electrode, which is less than 0.2 eV . The shift of the squared neutrino mass due to such an effect was estimated in [6]. According to the formula derived in this work, $\Delta m_\nu^2 = -2\sigma_E^2$. Thus, the shift of the neutrino mass squared is less than 0.08 eV^2 . It should be noted that the efficiency of the Si detector and the absolute value of the retarding potential on the spectrometer electrode do not affect the estimate of the mass because the normalization factor and the end point energy are free parameters.

Estimates of statistical and systematic errors were made for each run. To estimate the effect of the source thickness uncertainty, the following procedure was used for each run:

1. We fit the spectrum with an average value of the source thickness and estimate the squared neutrino mass $\langle m_\nu^2 \rangle$.
2. Then we fit with the thickness value shifted by its error ($\pm 3\%$) to get the new estimates for $\langle m_\nu^2 \rangle_{\pm shift}$.
3. The averaged difference $|\langle m_\nu^2 \rangle - \langle m_\nu^2 \rangle_{\pm shift}|$ is taken as a systematic uncertainty from the source thickness.
4. The systematic uncertainty from the trapping is calculated in a similar way.

A small error also comes from the processing of preliminary data. There, detector dead time and overlapping events are taken into account. Corrections for dead time and overlapping become visible only at relatively high count rates when the retarding potential is lower than 18400 V . These points were not used in the analysis of the spectrum.

The sources of systematic uncertainty are:

1. Uncertainty of source thickness.
2. Final state spectrum ambiguity.
3. Uncertainty in parameters of the trapping effect.
4. Instability of the retarding potential.

All errors are summed quadratically.

V. RESULTS

Results of the analysis are presented in Table I. Runs that were too short and runs where external parameters (mainly source thickness) could not be estimated with the required precision were not used in the analysis. In particular, run 21 (May 1997) and all the earlier runs were not included because there were no calibrations done with an electron gun, and consequently, the thickness value X_0 was unreliable.

The final result and systematic uncertainty were obtained by averaging over all runs weighted using statistical errors. Thus, systematic uncertainty for individual run does not affect the overall estimate of the neutrino mass squared. As a result we get

$$m_\nu^2 = -0.67 \pm 1.89_{stat} \pm 1.68_{syst} eV^2.$$

After summing errors in quadrature our estimate is

$$m_\nu^2 = -0.67 \pm 2.53 eV^2.$$

The result for the neutrino mass squared is negative but close to zero, within one sigma. For comparison, the result obtained earlier by our group [2] is $m_\nu^2 = -2.3 \pm 2.5_{stat} \pm 2.0_{syst} eV^2$, or $m_\nu^2 = -2.3 \pm 3.2 eV^2$. An improved precision of the current analysis comes from the usage of four free parameters in the fit (instead of six, as was done earlier with two additional parameters for a steplike structure) and an increase of the data amount. To decrease systematic uncertainties we also increase the low energy cut off of the data range from 18300 V to 18400 V.

Since the final m_ν^2 value is slightly negative, one can derive an upper physical bound for the neutrino mass. There is no single universal way to do this. Many experiments published the Bayesian limits which were calculated from the measured m_ν^2 value. It seems that for a value which is out of the physical region the most correct way would be to calculate the so-called sensitivity limit [11]. It uses error information but not the estimate itself; i.e., it is not sensitive to how negative the estimate is. In our case, this limit is calculated in the following way:

$$m_\nu^2 < 2.53 \times 1.96 = 4.96 eV^2, \text{ 95\% } C. L.,$$

where 1.96 is a standard multiplier for the 95% confidence level. For the neutrino mass this gives $m_\nu < 2.2 eV$. The corresponding value obtained by the Mainz group was $m_\nu < 2.4 eV$ [3].

The unified approach of Feldman and Cousins [12] and Bayesian methods yield the following upper limits for m_ν :

$$\begin{aligned} m_\nu &< 2.12 eV, \text{ 95\% } C. L. \text{ Bayesian,} \\ m_\nu &< 2.05 eV, \text{ 95\% } C. L. \text{ Feldman and Cousins.} \end{aligned}$$

The coincidence of our neutrino mass upper limit in the Feldman and Cousins approach with the result presented

in 2003 [2] is accidental. In the current analysis the final error is smaller, but $m_\nu^2 = -0.67 \pm 2.53 eV^2$ is less negative compared to the value of $m_\nu^2 = -2.3 \pm 3.2 eV^2$ in [2].

We also want to stress that in our analysis there is no need for any additional structure, like a step, at the upper end of the β -electron spectrum, which made an unambiguous interpretation difficult. To confirm this, we performed additional fits with two extra parameters in an attempt to reproduce a steplike structure, as was done in the old analysis [2]. In the last column of Table I we present $\chi^2_S/d.o.f.$ values for these fits. For run 33 the fit with the step did not converge despite all our attempts. There is no significant change in χ^2 values with such a step. Then, considering that the major difference between the two analyses is an estimate of the source thickness, for two runs we manually decreased the source thickness by a few percent to the value used in the old analysis. After that, the step reappears at about the same position from the spectrum's upper end and with a similar amplitude. Thus, we conclude that the reasons why the results of the new analysis differ from the old one are a more thorough and careful file selection and a more complete account of the experimental conditions.

VI. CONCLUSION

Data analysis was performed over a set of data taken from 1994 to 2004 by the Troitsk ν -mass experiment. Very early runs and a few runs taken after 1997 were rejected due to the lack of full information on experimental conditions or missing calibrations. The knowledge of the total column density in the windowless gaseous tritium source appeared to be the most critical. Some statistics were added from the runs which were excluded from the previous analysis.

For the analysis a new method of quasioptimal moments was used with Poisson statistics of experimental points with a low counting rate. An experimental estimate for the neutrino mass squared is $m_\nu^2 = -0.67 \pm 2.53 eV^2$. From this we obtain an upper sensitivity limit $m_\nu < 2.2 eV$, 95% *C. L.* and upper limit estimates $m_\nu < 2.12 eV$, 95% *C. L.* for Bayesian statistics, and $m_\nu < 2.05 eV$, 95% *C. L.* for the Feldman and Cousins approach. Within the present analysis, there is no statistically significant indication of a structure at the end of the spectrum.

With deep regret we have to say that during preparation of this paper the actual leader of the experiment, the world recognized expert on neutrino mass measurements Vladimir Lobashev passed away.

VII. ACKNOWLEDGMENTS

This work was supported by the Russian Foundation for Basic Research under Grants No. 93-02-039-03-a,

Run	Date month.year	m_ν^2	σ_{stat}	σ_X	σ_{trap}	σ_{syst}	$\chi^2/d.o.f.$	$\chi_S^2/d.o.f.$
22	06.1997	-7.55	9.89	1.1	0.34	1.34	0.796	0.814
23	12.1997	2.53	4.57	1.31	0.352	1.52	1.043	1.07
24, first part	01.1998	-1.31	4.32	1.35	0.318	1.55	0.923	0.964
24, second part	02.1998	-5.44	4.98	1.48	0.342	1.67	1.026	1.041
25	06.1998	-0.11	7.35	1.57	0.378	1.76	0.847	0.739
28	05.1999	2.60	6.99	1.82	0.4	1.99	1.421	1.496
29	10.1999	-0.51	7.50	1.94	0.416	2.10	1.268	1.456
30	12.1999	3.14	8.31	2.04	0.434	2.19	1.523	1.327
31	12.2000	-8.06	6.99	1.45	0.38	1.65	0.902	0.943
33	06.2001	7.21	8.82	1.47	0.504	1.70	1.378	
36	04.2002	1.91	6.72	1.37	0.322	1.57	1.356	1.379

TABLE I: Results for the neutrino squared mass estimate for different runs. All values are in eV^2 . Total systematic uncertainties are shown in the seventh column. The next to last column represents $\chi^2/d.o.f.$ obtained in each fit. The last column, $\chi_S^2/d.o.f.$, demonstrates how much the χ^2 value changes by introducing an additional steplike structure as was done in the previous analysis [2].

No. 96-02-18633-a, 02-00459-a, No. 05-02-17238-a, No. 08-02-00459-a, and grant from International Science and Technology Center, No. 1076. We also would like to thank our colleagues N. A. Golubev, O. V. Kazachenko, B. M. Ovchinnikov, N. A. Titov, Yu. I. Zakharov, and I.

E. Yarykin for their valuable contribution to the experiment preparation and data taking. Special thanks go to Ernst Otten and Christian Weinheimer for their interest and useful discussions of the results.

[1] K. Nakamura et al., (Particle Data Group), J. Phys. G **37**, 075021 (2010).
[2] V.M. Lobashev, Nucl. Phys. A **719**, 153c (2003).
[3] Ch. Kraus et al., Eur. Phys. J. C **40**, 447 (2005).
[4] F.V. Tkachov, arXiv:physics/0604127.
[5] F. James, CERN Program Library Long Writeup D **506**, (1994).
[6] R.G.H. Robertson and D. Knapp, Annu. Rev. Nucl. Part. Sci. **38**, 185 (1988).
[7] M. Donszelmann et al., J. Phys.: Conf. Series, **119**,

032016 (2008).
[8] J.J. Simpson, Phys. Rev. D **23**, 649 (1981).
[9] S. Jonsell and H.J. Monkhorst, Phys. Rev. Lett. **76**, 4476 (1996).
[10] V.N. Aseev et al., Eur. Phys. J. D **10**, 39 (2000).
[11] F.V. Tkachov, arXiv:physics/0911.4271.
[12] G.J. Feldman and R.D. Cousins, Phys. Rev. D **57**, 3873 (1998).